applied sciences

MDPI

Article

The Optimization of Covert Communication in Asymmetric Jammer—Assist Systems

Sen Qiao, Ruizhi Zhu, Xiaopeng Ji *, Junjie Zhao and Huihui Ding

School of Electronics and Information Engineering, Nanjing University of Information Science and Technology, Nanjing 210044, China
* Correspondence: jixiaopeng@nuist.edu.cn

Abstract: This research investigates the feasibility of covert and reliable communication between Alice and Bob in the presence of a vigilant adversary, Willie, employing a jammer in a complex Gaussian channel. Alice strategically manipulates the noise-power ratio along the real and imaginary axes to disrupt Willie's detection capabilities. Covertness constraints are quantified using KL divergence, and transmission performance is assessed through mutual information. Additionally, an optimization method is introduced to enhance covert communication by fine-tuning the amplitude gain and noise-power ratio. Numerical results confirm the effectiveness and superiority of the proposed method, showcasing its ability to maximize covert transmission rates.

Keywords: covertcommunication; asymmetric jammer; binary phase shift keying; Taylor series expansion

Citation: Qiao, S.; Zhu, R.; Ji, X.; Zhao, J.; Ding, H. The Optimization of Covert Communication in Asymmetric Jammer−Assist Systems. *Appl. Sci.* **2024**, *14*, 483. https://doi.org/10.3390/app14020483

Academic Editor: Gianluigi Ferrari

Received: 11 December 2023
Revised: 31 December 2023
Accepted: 4 January 2024
Published: 5 January 2024

1. Introduction

Secure communication has traditionally centered on preventing adversaries from deciphering message content [1–4]. However, in the realm of wireless communication, traditional information security measures prove inadequate to meet current security demands [5,6]. Even when information is encrypted, the potential leakage of sensitive data through metadata, such as network traffic patterns, poses a significant concern [7].

The imperative to conceal communication behaviors has prompted the development of covert communication technology [8]. In scenarios like battlefield environments or confrontational situations, the slightest indication of exposed communication intentions can lead to significant strategic failures [5]. Consequently, the military has devised diverse techniques, including the spread spectrum technique [6,9,10], to ensure the covertness of communication, aiming to hide its presence from vigilant adversaries. Despite the multitude of proposed covert communication methods, such as encoding information onto the training sequences of WiFi [11], utilizing the cyclic prefix of WiFi OFDM symbols [12], or manipulating a perturbed WiFi QPSK constellation [13], the overarching goal remains the formulation of strategies that effectively obfuscate communication activities in high-stakes environments.

Recent research has pivoted towards the pursuit of reliable covert communication, necessitating that Willie's detection error in discerning Alice's transmission to Bob approaches random guessing, while Bob's error in recovering Alice's message becomes exceedingly small [14]. Specifically, when employing additive white Gaussian noise (AWGN) channels for both the Alice-to-Bob and Alice-to-Willie communication paths, *square root law* (SRL) was established by [8,15]. This SRL stipulates that, with a sufficiently lengthy pre-shared secret between Alice and Bob, covert communication can be achieved by constraining the per-symbol power to $\mathcal{O}(\frac{1}{\sqrt{n}})$, which diminishes to 0 as n increases. As a consequence, Ref. [8] demonstrated the transmission of $\mathcal{O}(\sqrt{n})$ bits (and no more) within n channel uses. Subsequent research has delved into various aspects, including the determination

of the pre-shared secret's optimal length in [16,17], the characterization of constants concealed by Big-$\mathcal{O}$ notation in [17,18], and the theoretical and experimental exploration of covert communication over quantum channels in [19]. Moreover, this seminal theorem has subsequently been extended to various channel models, including discrete memoryless channels [17,18,20], binary symmetric channels [16] and multiuser channels [21–25], etc.

In traditional covert communication theory research, significant attention has been devoted to exploring theoretical boundaries over real Gaussian channels. The work presented in [9] expands the scope of covert communication theoretical research to encompass complex Gaussian channels, substantiating the boundary of covert communication over such channels. Existing works have investigated covert communication with random noise [26] and jammers [14,27]. Subsequently, jammer-aided covert communication were extended to UAV communication [28] and backscatter communication [29]. However, existing research on the theoretical boundaries of covert communication has been conducted in the context of real Gaussian channels, and for computational simplicity and optimization convenience, Gaussian input has been employed as the channel input. Nevertheless, in practical communication scenarios, the scenario of using Binary Phase Shift Keying (BPSK) as the channel input in a complex Gaussian channel has not been considered. In this work, we consider covert communication over complex Gaussian channels in the presence of an uninformed jammer. It is worth noting that jammer and Alice do not coordinate fully, similar to the scenario in [14]. As shown in Figure 1, the jammer sends asymmetric complex Gaussian noise signals, interfering with Willie's covert communication detection. Alice can only control the signal allocation ratio of the jammer, i.e., the power ratio of noise on the real and imaginary axes. Willie cannot demodulate the jamming noise, but Willie can know the power ratio of complex Gaussian noise on the real and imaginary axes in the environment. Regarding Bob, we consider two scenarios: in one case, Bob can perfectly demodulate the jamming noise from the jammer, thereby eliminating interference. In the other case, Bob cannot fully demodulate the jamming noise from the jammer but can partially mitigate the noise interference introduced by the jammer.

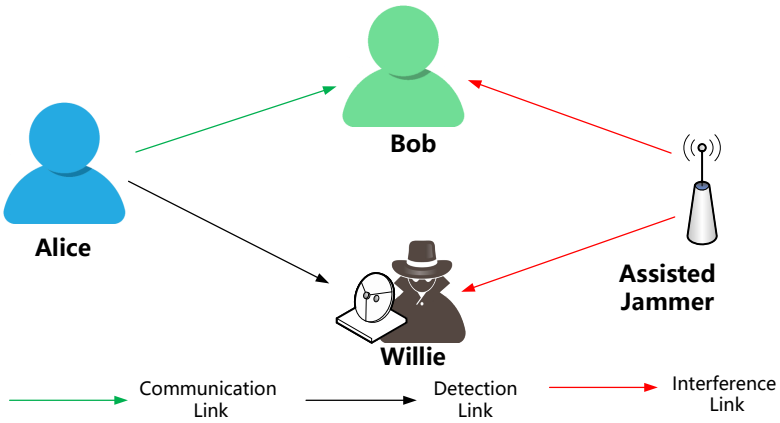

Figure 1. Covert communication in jammer−assist systems.

Our principal contributions can be succinctly summarized as follows:

(1) We explore covert communication in a scenario with a partially cooperative jammer within a complex Gaussian channel. KL divergence serves as our metric for covertness, while mutual information quantifies the transmission rate.

(2) We adopt BPSK input instead of Gaussian input, enhancing the applicability of our theory in real-world communication systems and bolstering the feasibility of our approach.

(3) Employing Taylor series expansion, we approximate KL divergence and mutual information under BPSK input. Transforming the dual-parameter optimization problem involving transmission amplitude gain and noise allocation ratio into a single-parameter optimization task significantly simplifies the complexity of the optimization process.

(4) Through numerical simulations, we validate our proposed method and theory. The precision of the Taylor approximation and the efficacy of the single-parameter optimization are confirmed, providing robust evidence for the validity of our proposed approach.

The remainder of this paper is organized as follows. In Section 2, the modeling of asymmetric noise communication scenarios is introduced, encompassing a scenario overview and problem formalization. In Section 3, the performance analysis of covert communication is provided, including transmission rates and covertness performance. In Section 4, the optimization method of transmission amplitude and noise power ratio is proposed. Section 5 presents numerical simulations to evaluate the outcomes of the optimization. Finally, Section 6 provides the conclusion and summary of the paper.

2. System Model

2.1. Communication Scenario

As shown in Figure 1, we consider a wireless covert communication scenario with the assistance of a jammer, involving a covert information transmitter (Alice), a covert information receiver (Bob), a covert communication detector (Willie), and a jammer assisting Alice in covert transmission. Alice, Bob, and Willie are equipped with a single antenna. We consider a quasi-static block fading model where the channel is static and frequency-flat within each coherent interval containing n symbols. The signal received by Bob and Willie can be expressed as

$$\hat{Z}_b = h_b D + n_{j,b} + \hat{n}_b, \tag{1}$$

$$\hat{Z}_w = h_w D + n_{j,w} + \hat{n}_w, \tag{2}$$

respectively, where $D \in \mathbb{C}$ is the transmitted signal, and $h_b \in \mathbb{C}$ and $h_w \in \mathbb{C}$ are Alice-to-Bob and Alice-to-Willie channel coefficient, which are assumed acceptable to everyone. $n_{j,b}$ and $n_{j,w}$ denote the interference signals received from jammer at Bob and Willie, both of which are composed of the zero-mean complex-valued Gaussian noise vectors. And $\hat{n}_b \in \mathbb{C}$ and $\hat{n}_w \in \mathbb{C}$ denote the zero-mean complex-valued Gaussian noise vectors with the covariance $2\hat{\sigma}_b^2$ and $2\hat{\sigma}_w^2$. Instead of adopting the conventional assumption of Gaussian input data, we let D be the symbol randomly selected from well-known BPSK constellations set with amplitude gain β, i.e., $\{-\beta, +\beta\}$. In practical communication systems, BPSK modulation is favored over Gaussian modulation due to its simplicity and efficiency [5,8,30]. In contrast, Gaussian modulation introduces complexity with a continuum of signal states, making it less practical for many communication scenarios. Considering the composition of jammer interference signals, we can equivalently rewrite the channel as

$$Z_b = h_b D + n_b, \tag{3}$$

$$Z_w = h_w D + n_w, \tag{4}$$

where $n_b \sim \mathcal{CN}(0, \sigma_b^2)$ and $n_w \sim \mathcal{CN}(0, \sigma_w^2)$ denote the equivalent noise after superimposing the interference signals. In the following context, we will analyze and optimize our problem based on equivalent channels (3) and (4).

2.2. Transmission Scheme

Alice encode a message M into a codeword $D^n = \left[D_1, ..., D_n\right] \in \mathbb{C}^n$ by random coding generation and i-th symbol D is independently drawn from $\{-\beta, \beta\}$ with equal probability [5,31]. The codeword D^n is generated independently and identically distribution (i.i.d.) randomly as follows:

$$\mathbf{P}(D^n) = \prod_{i=1}^{n} P_D(D_i). \tag{5}$$

Bob employs his contextual understanding to decode the covert messages, based on the observation of $Z_b^n = [Zb, 1, ..., Zb, n] \in \mathbb{C}^n$. The quantification of the transmission rate

is accomplished through the assessment of mutual information between the discrete input D^n and the channel output Z_b^n, which is given by

$$\mathbb{I}(Zb^n; D^n) = \mathbb{I}(Zb, 1, ..., Zb, n; D_1, ..., D_n). \tag{6}$$

Bob possesses knowledge regarding the construction of the codebook, i.e., $\{-\beta, +\beta\}$, and he receives the symbols corrupted by AWGN. Then, we give the following joint distribution of Z_b^n and D^n as follows:

$$P(Z_b^n D^n) = \mathbf{P}_D^n(D^n) \times W_{Z_b^n|D^n}(Z_b^n|D^n). \tag{7}$$

where

$$P_{Z_b^n D^n}(x, y) = \frac{1}{2}\frac{1}{2\pi\sqrt{\sigma_{b,x}\sigma_{b,y}}}\left[\exp\left(-\frac{(x+h_{b,x}\beta)^2}{2\sigma_{b,x}^2} - \frac{(y+h_{b,y}\beta)^2}{2\sigma_{b,y}^2}\right) + \exp\left(-\frac{(x-h_{b,x}\beta)^2}{2\sigma_{b,x}^2} - \frac{(y-h_{b,y}\beta)^2}{2\sigma_{b,y}^2}\right)\right], \tag{8}$$

with $h_{b,x}$ and $h_{b,y}$ denote the channel coefficient of complex value h_b on x-axis and y-axis, $\sigma_{b,x}^2$ and $\sigma_{b,y}^2$ denote the variance of the complex Gaussian noise at Bob on the x-axis and y-axis.

2.3. Hypothesis Test

Willie conducts a binary hypothesis test [8] based on n consecutive observations $Z_w^n = [Zw, 1, ..., Zw, n] \in \mathbb{C}^n$ to ascertain whether Alice is communicating to Bob. The total power of the jammer remains constant P_J, but Alice can adjust the power distribution ratio α of the jammer's output signals along the real and imaginary axes. Specifically, the jammer's power on the x-axis is αP_j, and on the y-axis, it is $(1-\alpha)P_j$. Due to the differing noise power along the two axes, this configuration results in an asymmetric jammer. Let $\sigma_{w,x,0}^2$ and $\sigma_{w,y,0}^2$ denote the variance of the complex Gaussian noise at Willie on the x-axis and y-axis. Specifically, the null hypothesis ($\mathcal{H}_0$) posits the absence of communication, where each sample $Zw, i = n_{w,i}$ is an independent and identically distributed (i.i.d.) complex-Gaussian random variable following the distribution $\mathcal{CN}(0, \sigma_a^2)$ with $\sigma_a^2 = \sigma_{w,x,0}^2 + \sigma_{w,y,0}^2 + P_J$. On the other hand, the alternative hypothesis ($\mathcal{H}_1$) suggests communication is occurring, and each sample $Zw, i = h_w D_i + n_{w,i}$. Willie's objective is to discriminate between these two hypotheses:

$$\mathcal{H}_0: \quad Zw = n_w, \tag{9}$$

$$\mathcal{H}_1: \quad Z_w = h_w D + n_w, \tag{10}$$

where h_w is the channel coefficient from Alice to Willie. Let $\mathbb{P}_1^n$ (resp. $\mathbb{P}_0^n$) represent the input distribution corresponding to Willie's n observations under the conditions of $\mathcal{H}_1$ (resp. $\mathcal{H}_0$), respectively. The probability of *false alarm*, rejecting $\mathcal{H}_0$ when it is true, is denoted by $\mathcal{P}_{FA}$, while the probability of *missed detection*, accepting $\mathcal{H}_0$ when it is false, is denoted by $\mathcal{P}_{MD}$. Willie has knowledge of the distributions $\mathbb{P}_1^n$ and $\mathbb{P}_0^n$, and can conduct an optimal statistical hypothesis test such that $\mathcal{P}_{FA} + \mathcal{P}_{MD} \geq 1 - \sqrt{\mathcal{D}(\mathbb{P}_1^n \| \mathbb{P}_0^n)}$, where $\mathcal{D}(\mathbb{P}_1^n \| \mathbb{P}_0^n)$ represents the KL divergence between $\mathbb{P}_1^n$ and $\mathbb{P}_0^n$. The objective is to achieve covert communication by ensuring that the sum of error probabilities is one, i.e., $\mathcal{P}_{FA} + \mathcal{P}_{MD} = 1$. This implies making $\mathcal{D}(\mathbb{P}_1^n \| \mathbb{P}_0^n)$ negligible [32–34], specifically by guaranteeing that the KL divergence satisfies the condition

$$\mathcal{D}(\mathbb{P}_1^n \| \mathbb{P}_0^n) \leq \epsilon, \tag{11}$$

where ϵ is an arbitrarily small value within the range (0,1).

Willie possesses knowledge regarding the construction of the codebook and jammer noise, both the set of all potential discrete constellation sets and input distribution, and he receives the symbols corrupted by AWGN. The distribution of $\mathbb{P}_{0,w}$ can be expressed as

$$\mathbb{P}_0(x,y) = \frac{1}{2\pi\sqrt{(\sigma_{w,x,0}^2+\alpha P_J)(\sigma_{w,y,0}^2+(1-\alpha)P_J))}} \times \exp\Big(-\frac{x^2}{2(\sigma_{w,x,0}^2+\alpha P_J)} - \frac{y^2}{2(\sigma_{w,y,0}^2+(1-\alpha)P_J)}\Big). \tag{12}$$

Similarly, The distribution of $\mathbb{P}_{1,w}^n$ can be expressed as

$$\mathbb{P}_1(x,y) = \frac{1}{2}\frac{1}{2\pi\sqrt{(\sigma_{w,x,0}^2+\alpha P_J)(\sigma_{w,y,0}^2+(1-\alpha)P_J)}} \times \Bigg[\exp\Big(-\frac{(x-h_{w,x}\beta)^2}{2(\sigma_{w,x,0}^2+\alpha P_J)} - \frac{(y-h_{w,y}\beta)^2}{2(\sigma_{w,y,0}^2+(1-\alpha)P_J)}\Big) + \exp\Big(-\frac{(x+h_{w,x}\beta)^2}{2(\sigma_{w,x,0}^2+\alpha P_J)} - \frac{(y+h_{w,y}\beta)^2}{2(\sigma_{w,y,0}^2+(1-\alpha)P_J)}\Big)\Bigg], \tag{13}$$

where $h_{w,x}$ and $h_{w,y}$ denote the channel coefficient of complex value h_w on x-axis and y-axis.

2.4. Problem Formulation

In this work, we aim to investigate the transmission design with the goal of maximizing the mutual information in (6) while adhering to the covertness constraint stipulated in (11). Our focus lies in the optimization of the amplitude gain β and the jammer noise distribution ratio α on the x-axis and y-axis. The problem of covert communication in jammer−assist systems is formulated as:

$$\text{P1}: \max_{\beta,\alpha} \quad \mathbb{I}(Z_b^n; D^n) \tag{14}$$

$$\text{s.t.} \quad \mathcal{D}(\mathbb{P}_1^n \| \mathbb{P}_0^n) \le \epsilon, \tag{15}$$

$$0 < \beta, \tag{16}$$

$$0 < \alpha < 1. \tag{17}$$

3. Design of Amplitude Gain and Jammer Noise Distribution

To compute the optimal jammer noise allocation ratio, we define

$$\sigma_a^2 \triangleq \sigma_{w,x}^2 + \sigma_{w,y}^2 \tag{18}$$

$$\sigma_{w,x}^2 \triangleq \mu\sigma_a^2 = \sigma_{w,x,0}^2 + \alpha P_J, \tag{19}$$

$$\sigma_{w,y}^2 \triangleq (1-\mu)\sigma_a^2 = \sigma_{w,y,0}^2 + (1-\alpha)P_J, \tag{20}$$

where $0 < \mu < 1$ is a auxiliary parameters. Combining with (12) and (13), we have

$$\mathbb{P}_0(x,y) = \frac{1}{2\pi\sigma_{w,x}\sigma_{w,y}} \exp\Big(-\frac{x^2}{2\sigma_{w,x}^2} - \frac{y^2}{2\sigma_{w,y}^2}\Big) \tag{21}$$

$$\mathbb{P}_1(x,y) = \frac{1}{2}\frac{1}{2\pi\sigma_{w,x}\sigma_{w,y}} \Bigg[\exp\Big(-\frac{(x-h_{w,x}\beta)^2}{2\sigma_{w,x}^2} - \frac{(y-h_{w,y}\beta)^2}{2\sigma_{w,y}^2}\Big) + \exp\Big(-\frac{(x+h_{w,x}\beta)^2}{2\sigma_{w,x}^2} - \frac{(y+h_{w,y}\beta)^2}{2\sigma_{w,y}^2}\Big)\Bigg]. \tag{22}$$

Then, the problem P1 can be reformulated as

$$\text{P2}: \max_{\beta,\mu} \quad \mathbb{I}(Z_b^n; D^n) \tag{23}$$

$$\text{s.t.} \quad (15),\ (16),$$

$$\min\{\frac{\sigma_{w,x,0}^2}{\sigma_a^2}, \frac{\sigma_{w,y,0}^2}{\sigma_a^2}\} \leq \mu \leq \max\{\frac{\sigma_{w,x,0}^2 + P_J}{\sigma_a^2}, \frac{\sigma_{w,y,0}^2 + P_J}{\sigma_a^2}\}. \tag{24}$$

The KL divergence between $\mathbb{P}_1$ and $\mathbb{P}_0$ can expressed as

$$\mathcal{D}(\mathbb{P}_1 \| \mathbb{P}_0) = \iint_{-\infty}^{\infty} \mathbb{P}_1(x,y) \log \frac{\mathbb{P}_1(x,y)}{\mathbb{P}_0(x,y)} \mathrm{d}x\mathrm{d}y \tag{25}$$

where

$$\log \frac{\mathbb{P}_1(x,y)}{\mathbb{P}_0(x,y)} = \log \frac{1}{2} \Bigg[\exp\Big(- \frac{{h_{w,x}}^2\beta^2 - 2xh_{w,x}\beta}{2\sigma_{w,x}^2} - \frac{{h_{w,y}}^2\beta^2 - 2h_{w,y}\beta}{2\sigma_{w,y}^2} \Big) + \exp\Big(- \frac{{h_{w,x}}^2\beta^2 + 2xh_{w,x}\beta}{2\sigma_{w,x}^2} - \frac{{h_{w,y}}^2\beta^2 + 2h_{w,y}\beta}{2\sigma_{w,y}^2} \Big) \Bigg]. \tag{26}$$

Performing Taylor expansion, we can obtain

$$\log \frac{\mathbb{P}_1(x,y)}{\mathbb{P}_0(x,y)} = Z_1\beta^2 + Z_2\beta^4 + \mathcal{O}(\beta^5), \tag{27}$$

where

$$Z_1 = -\frac{{h_{w,x}}^2}{2\sigma_{w,x}^2} - \frac{{h_{w,y}}^2}{2\sigma_{w,y}^2} + \frac{h_{w,x}h_{w,y}xy}{\sigma_{w,x}^2\sigma_{w,y}^2} + \frac{{h_{w,y}}^2y^2}{2\sigma_{w,y}^4} + \frac{{h_{w,x}}^2x^2}{2\sigma_{w,x}^4}, \tag{28}$$

$$Z_2 = -\frac{{h_{w,x}}^4x^4}{12\sigma_{w,x}^8} - \frac{{h_{w,y}}^4y^4}{12\sigma_{w,y}^8} - \frac{{h_{w,x}}^2{h_{w,y}}^2}{2\sigma_{w,x}^4\sigma_{w,y}^4} - \frac{{h_{w,x}}^3h_{w,y}x^3y}{3\sigma_{w,x}^6\sigma_{w,y}^2} - \frac{h_{w,x}{h_{w,y}}^3xy^3}{3\sigma_{w,x}^2\sigma_{w,y}^6}. \tag{29}$$

Combining with (27)–(29), Equation (25) can be rewritten as

$$\mathcal{D}(\mathbb{P}_1 \| \mathbb{P}_0) = \iint_{-\infty}^{\infty} \mathbb{P}_1(x,y)\Big(Z_1\beta^2 + Z_2\beta^4 + \mathcal{O}(\beta^5)\Big)\mathrm{d}x\mathrm{d}y. \tag{30}$$

With some calculations, we can obtain

$$\iint_{-\infty}^{\infty} \mathbb{P}_1(x,y)Z_1\beta^2\mathrm{d}x\mathrm{d}y = -\frac{{h_{w,x}}^2\beta^2}{2\sigma_{w,x}^2} - \frac{{h_{w,y}}^2\beta^2}{2\sigma_{w,y}^2} + \frac{h_{w,x}^2h_{w,y}^2\beta^4}{\sigma_{w,x}^2\sigma_{w,y}^2} + \frac{{h_{w,y}}^2\beta^2(\sigma_{w,y}^2 + {h_{w,y}}^2\beta^2)}{2\sigma_{w,y}^4} + \frac{{h_{w,x}}^2\beta^2(\sigma_{w,x}^2 + {h_{w,x}}^2\beta^2)}{2\sigma_{w,x}^4} + \mathcal{O}(\beta^5). \tag{31}$$

and

$$\iint_{-\infty}^{\infty} \mathbb{P}_1(x,y)Z_2\beta^4\mathrm{d}x\mathrm{d}y = -\frac{3{h_{w,x}}^4\sigma_{w,x}^4\beta^4}{12\sigma_{w,x}^8} - \frac{3{h_{w,y}}^4\sigma_{w,y}^4\beta^4}{12\sigma_{w,y}^8} - \frac{{h_{w,x}}^2{h_{w,y}}^2\sigma_{w,x}^2\sigma_{w,y}^2\beta^4}{2\sigma_{w,x}^4\sigma_{w,y}^4} + \mathcal{O}(\beta^5) \tag{32}$$

$$= -\frac{{h_{w,x}}^4\beta^4}{4\sigma_{w,x}^4} - \frac{{h_{w,y}}^4\beta^4}{4\sigma_{w,y}^4} - \frac{{h_{w,x}}^2{h_{w,y}}^2\beta^4}{2\sigma_{w,x}^2\sigma_{w,y}^2} + \mathcal{O}(\beta^5) \tag{33}$$

Then, the KL divergence between $\mathbb{P}_1$ and $\mathbb{P}_0$ can be expressed as

$$\mathcal{D}(\mathbb{P}_1\|\mathbb{P}_0) = \frac{\beta^4}{4}\Big(\frac{{h_{w,x}}^2}{\sigma_{w,x}^2} + \frac{{h_{w,y}}^2}{\sigma_{w,y}^2}\Big)^2 + \mathcal{O}(\beta^5). \tag{34}$$

Combining with (19) and (20), the KL divergence can be expressed as

$$\mathcal{D}(\mathbb{P}_1^n\|\mathbb{P}_0^n) = \frac{n\beta^4}{4}\Big(\frac{{h_{w,x}}^2}{\mu\sigma_a^2} + \frac{{h_{w,y}}^2}{(1-\mu)\sigma_a^2}\Big)^2 + \mathcal{O}(\beta^5). \tag{35}$$

We can minimize $\mathcal{D}(\mathbb{P}_1\|\mathbb{P}_0)$ by minimizing

$$F(\mu) = \frac{{h_{w,x}}^2}{\mu\sigma_a^2} + \frac{{h_{w,y}}^2}{(1-\mu)\sigma_a^2}. \tag{36}$$

4. Analysis of the Transmission Rate

In this section, we will analyze the transmission rate of covert communication with mutual information. Specifically, we consider two cases: (1) Bob can perfectly eliminate the influence of interference; and (2) Bob can partially eliminate the influence of interference.

4.1. Derivation of Mutual Information at Bob

For the two cases we mentioned, the mutual information in (6) can be expressed as

$$\mathbb{I}(Zb^n; D^n) = n\mathbb{I}(Z_b; D). \tag{37}$$

Considering the codebook in Section 2.2, we have

$$\mathrm{I}(Z_b; D) = \mathrm{H}(Z_b) - \mathrm{H}(Z_b|D) \tag{38}$$

$$= -\iint p_b(x,y)\log p_b(x,y)\mathrm{d}x\mathrm{d}y + \iint \sum_{i=1}^{2}\frac{1}{2}p_{b,i}(x,y)\log p_{b,i}(x,y)\mathrm{d}x\mathrm{d}y \tag{39}$$

$$= -\iint \sum_{j=1}^{2}\frac{1}{2}p_{b,j}(x,y)\log\Big[\sum_{i=1}^{2}\frac{1}{2}p_{b,i}(x,y)\Big]\mathrm{d}x\mathrm{d}y + \iint \sum_{j=1}^{2}\frac{1}{2}p_{b,j}(x,y)\log p_{b,j}(x,y)\mathrm{d}x\mathrm{d}y \tag{40}$$

$$= -\iint \sum_{j=1}^{2}\frac{1}{2}p_{b,j}(x,y)\log\Big[\frac{\sum_{i=1}^{2}\frac{1}{2}p_{b,i}(x,y)}{p_{b,j}(x,y)}\Big]\mathrm{d}x\mathrm{d}y, \tag{41}$$

where

$$p_{b,1}(x,y) = \frac{1}{2\pi\sigma_b^2}\left[\exp\Big(-\frac{(x+h_{b,x}\beta)^2}{2\sigma_{b,x}^2} - \frac{(y+h_{b,y}\beta)^2}{2\sigma_{b,y}^2}\Big)\right], \tag{42}$$

$$p_{b,2}(x,y) = \frac{1}{2\pi\sigma_b^2}\left[\exp\Big(-\frac{(x-h_{b,x}\beta)^2}{2\sigma_{b,x}^2} - \frac{(y-h_{b,y}\beta)^2}{2\sigma_{b,y}^2}\Big)\right]. \tag{43}$$

Performing Taylor expansion, we have

$$\log\left[\frac{\sum_{i=1}^{2}\frac{1}{2}p_{b,i}(x,y)}{p_{b,1}(x,y)}\right] = \beta\Big(\frac{h_{b,x}x}{\sigma_{b,x}^2} + \frac{h_{b,y}y}{\sigma_{b,y}^2}\Big) + \beta^2\Big(\frac{h_{b,x}^2x^2}{2\sigma_{b,x}^4} + \frac{h_{b,y}y^2}{2\sigma_{b,y}^4} + \frac{h_{b,x}h_{b,y}xy}{\sigma_{b,x}^2\sigma_{b,y}^2}\Big) + \mathcal{O}(\beta^3), \tag{44}$$

and

$$\log\left[\frac{\sum_{i=1}^{2}\frac{1}{2}p_{b,i}(x,y)}{p_{b,2}(x,y)}\right]=-\beta\Big(\frac{h_{b,x}x}{\sigma_{b,x}^2}+\frac{h_{b,y}y}{\sigma_{b,y}^2}\Big)+\beta^2\Big(\frac{h_{b,x}^2x^2}{2\sigma_{b,x}^4}+\frac{h_{b,y}y^2}{2\sigma_{b,y}^4}+\frac{h_{b,x}h_{b,y}xy}{\sigma_{b,x}^2\sigma_{b,y}^2}\Big)+\mathcal{O}(\beta^3). \tag{45}$$

With some calculations, we can obtain

$$\begin{aligned}&\iint\sum_{j=1}^{2}\frac{1}{2}p_{b,j}(x,y)\log\left[\frac{\sum_{i=1}^{2}\frac{1}{2}p_{b,i}(x,y)}{p_{b,j}(x,y)}\right]\mathrm{d}x\mathrm{d}y\\&=-\Big(\frac{h_{b,x}^2\beta}{\sigma_{b,x}^2}+\frac{h_{b,y}^2\beta}{\sigma_{b,y}^2}\Big)\beta+(\frac{h_{b,x}^2}{2\sigma_{b,x}^2}+\frac{h_{b,y}^2}{2\sigma_{b,y}^2})\beta^2+\mathcal{O}(\beta^3) &(46)\\&=-\Big(\frac{h_{b,x}^2}{2\sigma_{b,x}^2}+\frac{h_{b,y}^2}{2\sigma_{b,y}^2}\Big)\beta^2+\mathcal{O}(\beta^3), &(47)\end{aligned}$$

and the mutual information can be expressed as

$$\mathbb{I}(Z_b;D)=\Big(\frac{h_{b,x}^2}{2\sigma_{b,x}^2}+\frac{h_{b,y}^2}{2\sigma_{b,y}^2}\Big)\beta^2+\mathcal{O}(\beta^3). \tag{48}$$

4.2. Problem Reformulation for Two Cases

To measure the influence of interference, we define

$$\sigma_{b,x}^2\triangleq\sigma_{b,x,0}^2+\alpha\Delta P_J, \tag{49}$$

$$\sigma_{b,y}^2\triangleq\sigma_{b,y,0}^2+(1-\alpha)\Delta P_J. \tag{50}$$

where ΔP_J denotes the jammer interference power after interference elimination.

Case 1: if Bob can perfectly eliminate the influence of interference, $\Delta P_J=0$. Taking the derivative of the function $F(\mu)$, the minimal value $F^*(\mu)$ can be obtained when

$$\mu^*=\frac{h_{w,x}}{h_{w,y}+h_{w,x}}. \tag{51}$$

Considering the range of μ given in (24), the minimization of the KL divergence can be achieved when

$$\mu^*=\begin{cases}\max\{\frac{\sigma_{w,x,0}^2+P_J}{\sigma_a^2},\frac{\sigma_{w,y,0}^2+P_J}{\sigma_a^2}\} & \max\{\frac{\sigma_{w,x,0}^2+P_J}{\sigma_a^2},\frac{\sigma_{w,y,0}^2+P_J}{\sigma_a^2}\}\le\frac{h_{w,x}}{h_{w,y}+h_{w,x}}\\ \frac{h_{w,x}}{h_{w,y}+h_{w,x}} & \min\{\frac{\sigma_{w,x,0}^2}{\sigma_a^2},\frac{\sigma_{w,y,0}^2}{\sigma_a^2}\}<\frac{h_{w,x}}{h_{w,y}+h_{w,x}}<\max\{\frac{\sigma_{w,x,0}^2+P_J}{\sigma_a^2},\frac{\sigma_{w,y,0}^2+P_J}{\sigma_a^2}\}\\ \min\{\frac{\sigma_{w,x,0}^2}{\sigma_a^2},\frac{\sigma_{w,y,0}^2}{\sigma_a^2}\} & \frac{h_{w,x}}{h_{w,y}+h_{w,x}}\le\min\{\frac{\sigma_{w,x,0}^2}{\sigma_a^2},\frac{\sigma_{w,y,0}^2}{\sigma_a^2}\}\end{cases} \tag{52}$$

Combining with (35), (36) and the optimal μ^*, the constraint (15) can be rewritten as

$$\frac{n\beta^4}{4}F^2(\mu^*)\le\epsilon, \tag{53}$$

and the optimal amplitude gain β^* is given by

$$\beta^*=\left(\frac{4\epsilon}{nF^2(\mu^*)}\right)^{\frac{1}{4}}. \tag{54}$$

Then, we can obtain the maximum mutual information as

$$\mathbb{I}^*(Zb^n; D^n) = \sqrt{\frac{4n\epsilon}{F^2(\mu^*)}}\left(\frac{h_{b,x}^2}{2\sigma_{b,x,0}^2} + \frac{h_{b,y}^2}{2\sigma_{b,y,0}^2}\right). \tag{55}$$

Case 2: Bob can partially eliminate the influence of interference, $\Delta P_J = \eta P_J$ where $\eta \in (0, 1)$ denotes the coefficient of Bob's interference cancellation capability. Combining with (19) and (20), the ratio α is given by

$$\alpha = \frac{\mu\sigma_a^2 - \sigma_{w,x,0}^2}{P_J}. \tag{56}$$

Then, the mutual information can be expressed as

$$\hat{\mathbb{I}}(Zb^n; D^n) = \sqrt{\frac{n\epsilon}{F^2(\mu)}}\left(\frac{h_{b,x}^2}{(\sigma_{b,x,0}^2 + \alpha\eta P_J)} + \frac{h_{b,y}^2}{(\sigma_{b,y,0}^2 + (1-\alpha)\eta P_J)}\right). \tag{57}$$

Combining with (23), (16), (17) and (24), the problem P2 can be equivalently transformed to

$$\text{P3}: \max_{\mu} \quad \hat{\mathbb{I}}(Zb^n; D^n) \tag{58}$$

$$\text{s.t.} \quad (24). \tag{59}$$

Clearly, the optimal value of μ^* and the maximization of mutual information can be effortlessly obtained through an iterative exploration algorithm for α^*. Then, we can obtain the optimal amplitude gain β^*, and the original problem P1 has been fully addressed.

5. Numerical Results

In this section, we initiate the validation of our proposed KL divergence and mutual information approximation methods, operating within two distinct scenarios that encompass diverse h_w and h_b channel coefficients, along with varying interferer total power levels. Following the confirmation of the precision of these approximation methods, we conduct a thorough performance analysis, assessing both covertness and transmission rate using our proposed methodology. Subsequently, we ascertain the optimal noise allocation ratio for interferers. Finally, through a comparative performance evaluation between the optimal interference noise allocation ratio and alternative ratios, we establish the efficacy and superiority of the optimization method we have introduced.

In Figure 2a, the graph illustrates the KL divergence versus amplitude gain (β). We compare two scenarios with distinct parameters: $h_{w,x,0} = h_{w,y,0} = 0.5$, $P_J = 3$ and $h_{w,x,0} = h_{w,y,0} = 0.3$, $P_J = 5$. As depicted in Figure 2a, with the increase in amplitude gain (β), KL divergence gradually increases, indicating a deterioration in covertness. The Taylor expansion results obtained for KL divergence exhibit high fidelity with the precise values as β increases, affirming the precision and effectiveness of our proposed method in characterizing KL divergence in covert communication. Figure 2b presents the KL divergence versus amplitude gain (β) graph. We compare two scenarios with parameters $h_{b,x,0} = h_{b,y,0} = 0.5$, $P_J = 3$, $\eta = 0.3$ and $h_{b,x,0} = h_{b,y,0} = 0.2$, $P_J = 5$, $\eta = 0.3$. As illustrated in Figure 2b, with the increase in amplitude gain (β), mutual information and transmission rate gradually increase. The Taylor expansion results for transmission rate exhibit high fidelity with the precise values as β increases, demonstrating the precision and effectiveness of our proposed method in characterizing transmission rate in covert communication.

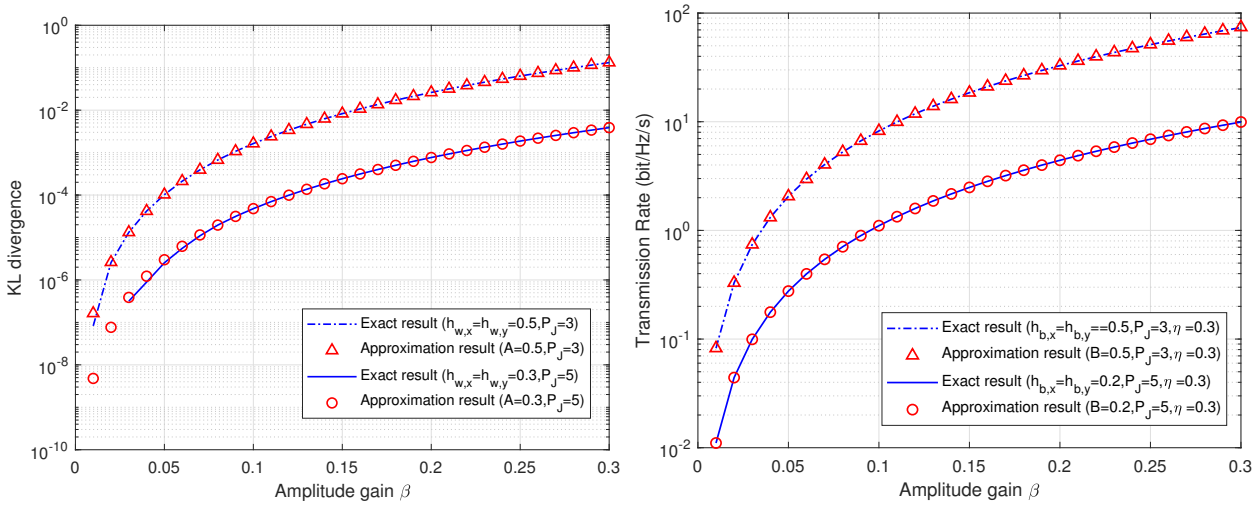

(**a**) (**b**)

Figure 2. Performance analysis of covert communication in jammer−assist system. (**a**) KL divergence versus amplitude gain. (**b**) Transmission rate versus amplitude gain.

In Figures 3 and 4, we design three distinct scenarios for comparative experiments. The parameters for the three scenarios are provided in Table 1.

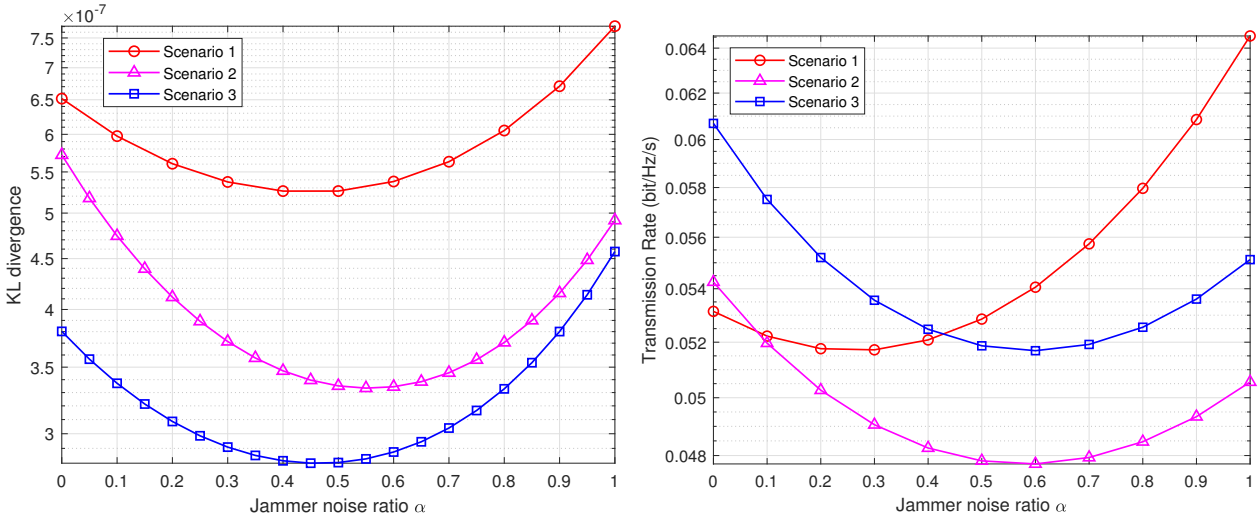

(**a**) (**b**)

Figure 3. Performance analysis of covert communication in jammer−assist system. (**a**) KL divergence versus jammer noise ratio. (**b**) Transmission rate versus jammer noise ratio.

In Figure 3a, Scenarios 1, 2, and 3 achieve optimal covertness ($\alpha = 0.48$, $\alpha = 0.58$, $\alpha = 0.45$, respectively) with minimal KL divergence values. In Figure 3b, Scenarios 1, 2, and 3 achieve maximum transmission rates ($\alpha = 1$, $\alpha = 0$, $\alpha = 0$, respectively). To obtain the globally optimal value for α that maximizes transmission rate under the same amplitude gain and covertness constraints, we utilize our proposed method and obtain the results of transmission rate versus noise allocation ratio α for the three scenarios.

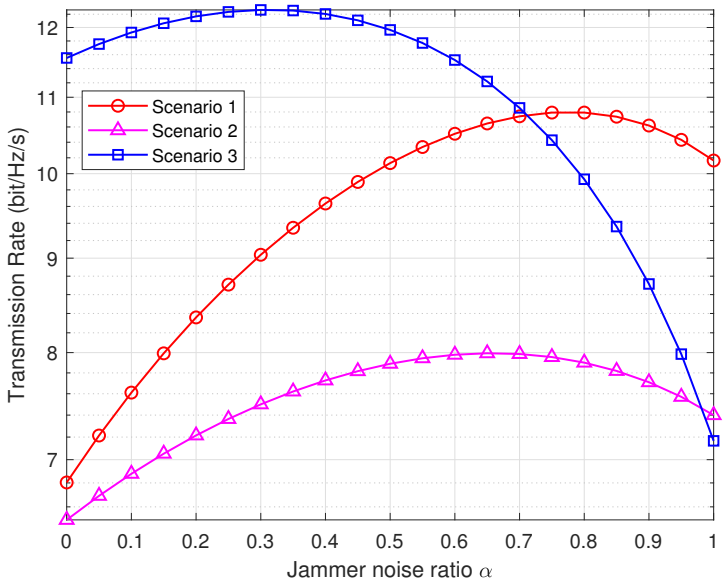

Figure 4. Transmission rate versus jammer noise ratio in three scenarios.

Table 1. Parameters for comparative experiments.

Scenario	P_J	$\sigma_{w,x,0}$	$\sigma_{w,y,0}$	$h_{w,x}$	$h_{w,y}$	η	$\sigma_{b,x,0}$	$\sigma_{b,y,0}$	$h_{b,x}$	$h_{b,y}$
1	5	3.5	2.5	0.46	0.38	0.3	3.8	2.2	0.22	0.56
2	5	4.5	3.5	0.45	0.44	0.3	3.5	2.0	0.41	0.52
3	5	5.5	1.5	0.15	0.13	0.3	2.8	4.2	0.15	0.18

As depicted in Figure 4, the results show the transmission rate versus noise allocation ratio α for $\beta = 0.1$. In Scenario 1, the maximum covert transmission rate is achieved at $\alpha = 0.78$; in Scenario 2, it is at $\alpha = 0.7$, and in Scenario 3, it is at $\alpha = 0.3$. Subsequently, based on the parameters of Scenario 3 and the obtained optimal noise allocation ratio $\alpha^* = 0.3$, we conduct a theoretical validation.

Figure 5a presents the KL divergence versus amplitude gain (β) results. We compare the results with the globally optimal allocation ratio $\alpha^* = 0.3$ against samples with $\alpha = 0.5$ and $\alpha = 0.8$. As β increases, $\alpha^* = 0.3$ consistently maintains optimal covertness (lower KL divergence values). Figure 5b displays the mutual information versus amplitude gain (β) results. We select the transmission rate at the globally optimal allocation ratio $\alpha^* = 0.3$ and compare it with samples at $\alpha = 0.5$ and $\alpha = 0.8$. As β increases, $\alpha = 0.8$ exhibits the lowest transmission rate. However, $\alpha = 0.5$ achieves a higher transmission rate than the globally optimal allocation ratio $\alpha^* = 0.3$. Considering the substantial degradation in covertness at $\alpha = 0.5$, further comparison under the same covertness constraints is necessary.

Figure 6 depicts the covert transmission rate versus covertness constraint ϵ. We select the results at the globally optimal allocation ratio $\alpha^* = 0.3$ and compare them with samples at $\alpha = 0.5$ and $\alpha = 0.8$. With an increasing covertness constraint ϵ, the covert transmission rate gradually increases. Under the same covertness constraint, $\alpha^* = 0.3$ attains the highest covert transmission rate. Combining the results from Figure 5a,b, our proposed optimization method achieves the globally optimal noise allocation ratio, realizing the maximum covert transmission rate under the same covertness constraints. Simulation results validate the effectiveness and superiority of our proposed method.

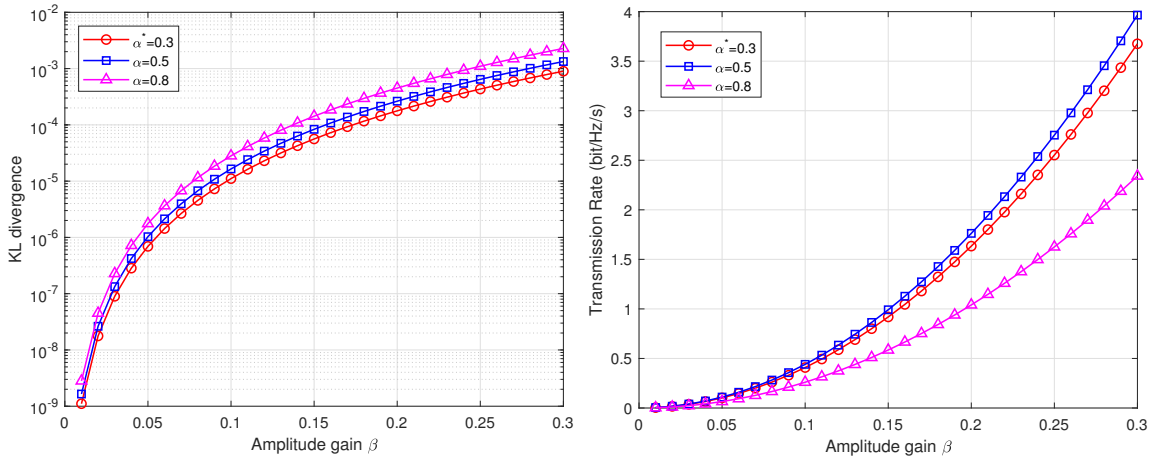

(**a**) (**b**)

Figure 5. Performance comparison of difference jammer noise ratio. (**a**) KL divergence versus amplitude gain. (**b**) Transmission rate versus amplitude gain.

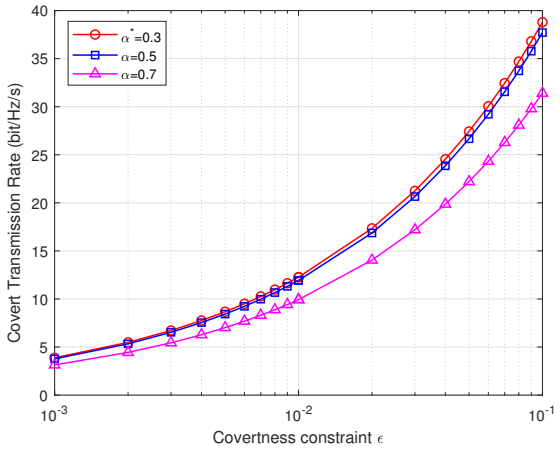

Figure 6. Covert transmission rate versus covertness constraint.

6. Conclusions

In this work, we investigate covert communication in a complex Gaussian channel with a partially coordinate jammer. Specifically, Alice aims to transmit covert information to Bob using BPSK codebook, while remaining undetected by Willie throughout the covert communication process. A jammer is present to assist Alice in covert communication, but Alice has limited control over the jammer, with adjustments constrained to the power allocation ratio along the real and imaginary axes in the complex Gaussian channel.

We employ KL divergence as a metric for covertness and mutual information as a metric for transmission rate. The optimization task involves adjusting both the amplitude of Alice's transmitted signal and the power allocation ratio of the jammer. Leveraging Taylor series expansion techniques, we approximate KL divergence and mutual information. Combining our approximation results, we degrade the complex dual-parameter optimization problem into a single-parameter traversal problem, simplifying the optimization complexity.

Numerical simulations validate the effectiveness of our proposed theory. In future work, we plan to extend the study to include different modulation schemes adopted by Alice, such as 16-QAM, 64-QAM, and other scenarios.

Author Contributions: Conceptualization, S.Q. and R.Z.; methodology, S.Q. and R.Z.; software, J.Z. and X.J.; validation, S.Q. and X.J.; writing—original draft preparation, H.D. and R.Z.; writing—review and editing, J.Z. and H.D.; visualization, H.D. and X.J.; supervision, S.Q. and J.Z.; funding acquisition, R.Z. All authors have read and agreed to the published version of the manuscript.

Funding: This research was funded by National Natural Science Foundation of China grant number U1836104, 61801073, 61931004, 62072250, National Key Research and Development Program of China grant number 2021QY0700, and The Startup Foundation for Introducing Talent of NUIST grant number 2021r039.

Institutional Review Board Statement: Not applicable.

Informed Consent Statement: Not applicable.

Data Availability Statement: The data presented in this study are available in the article.

Conflicts of Interest: The authors declare no conflicts of interest. The funders had no role in the design of the study; in the collection, analyses, or interpretation of data; in the writing of the manuscript; or in the decision to publish the results.

Abbreviations

The following abbreviations are used in this manuscript:

WIFI	Wireless Fidelity
OFDM	Orthogonal frequency-division multiplexing
BPSK	Binary Phase Shift Keying
AWGN	Additive White Gaussian Noise
QPSK	Quadrature Phase Shift Keying

References

1. Wu, Z.; Liu, R.; Shuai, H.; Zhu, S.; Li, C. Covert performance for integrated satellite multiple terrestrial relay networks with partial relay selection. *Sensors* **2022**, *22*, 5524. [CrossRef]
2. Moon, J. Performance Comparison of Relay-Based Covert Communications: DF, CF and AF. *Sensors* **2023**, *23*, 8747. [CrossRef]
3. Iqbal, A.; Al-Habashna, A.; Wainer, G.; Bouali, F.; Boudreau, G.; Wali, K. Deep Reinforcement Learning-Based Resource Allocation for Secure RIS-aided UAV Communication. In Proceedings of the 2023 IEEE 98th Vehicular Technology Conference (VTC2023-Fall), Hong Kong, China, 10–13 October 2023; pp. 1–6. [CrossRef]
4. Iqbal, A.; Tham, M.L.; Wong, Y.J.; Al-Habashna, A.; Wainer, G.; Zhu, Y.X.; Dagiuklas, T. Empowering Non-Terrestrial Networks With Artificial Intelligence: A Survey. *IEEE Access* **2023**, *11*, 100986–101006. [CrossRef]
5. Qiao, S.; Cao, D.; Zhang, Q.; Xu, Y.; Liu, G. Covert Communication Gains From Adversary's Uncertainty of Phase Angles. *IEEE Trans. Inf. Forensics Secur.* **2023**, *18*, 2899–2912. [CrossRef]
6. Bash, B.A.; Goeckel, D.; Towsley, D.; Guha, S. Hiding information in noise: Fundamental limits of covert wireless communication. *IEEE Commun. Mag.* **2015**, *53*, 26–31. [CrossRef]
7. Hu, J.; Lin, C.; Li, X. Relationship Privacy Leakage in Network Traffics. In Proceedings of the 2016 25th International Conference on Computer Communication and Networks (ICCCN), Waikoloa, HI, USA, 1–4 August 2016; pp. 1–9. [CrossRef]
8. Bash, B.A.; Goeckel, D.; Towsley, D. Limits of Reliable Communication with Low Probability of Detection on AWGN Channels. *IEEE J. Sel. Areas Commun.* **2013**, *31*, 1921–1930. [CrossRef]
9. Chen, X.; An, J.; Xiong, Z.; Xing, C.; Zhao, N.; Yu, F.R.; Nallanathan, A. Covert Communications: A Comprehensive Survey. *IEEE Commun. Surv. Tutor.* **2023**, *25*, 1173–1198. [CrossRef]
10. Çek, M.E.; Savaci, F. Stable non-Gaussian noise parameter modulation in digital communication. *Electron. Lett.* **2009**, *45*, 1256–1257. [CrossRef]
11. Classen, J.; Schulz, M.; Hollick, M. Practical covert channels for WiFi systems. In Proceedings of the 2015 IEEE Conference on Communications and Network Security (CNS), Florence, Italy, 28–30 September 2015; pp. 209–217. [CrossRef]
12. Grabski, S.; Szczypiorski, K. Steganography in OFDM Symbols of Fast IEEE 802.11n Networks. In Proceedings of the 2013 IEEE Security and Privacy Workshops, San Francisco, CA, USA, 23–24 May 2013; pp. 158–164. [CrossRef]
13. D'Oro, S.; Restuccia, F.; Melodia, T. Hiding Data in Plain Sight: Undetectable Wireless Communications Through Pseudo-Noise Asymmetric Shift Keying. In Proceedings of the IEEE INFOCOM 2019—IEEE Conference on Computer Communications, Paris, France, 29 April–2 May 2019; pp. 1585–1593. [CrossRef]
14. Sobers, T.V.; Bash, B.A.; Guha, S.; Towsley, D.; Goeckel, D. Covert communication in the presence of an uninformed jammer. *IEEE Trans. Wirel. Commun.* **2017**, *16*, 6193–6206. [CrossRef]

15. Bash, B.A.; Goeckel, D.; Towsley, D. Square root law for communication with low probability of detection on AWGN channels. In Proceedings of the 2012 IEEE International Symposium on Information Theory Proceedings, Cambridge, MA, USA, 1–6 July 2012; pp. 448–452.
16. Che, P.H.; Bakshi, M.; Jaggi, S. Reliable deniable communication: Hiding messages in noise. In Proceedings of the 2013 IEEE International Symposium on Information Theory, Istanbul, Turkey, 7–12 July 2013; pp. 2945–2949.
17. Bloch, M.R. Covert communication over noisy channels: A resolvability perspective. *IEEE Trans. Inf. Theory* **2016**, *62*, 2334–2354. [CrossRef]
18. Wang, L.; Wornell, G.W.; Zheng, L. Fundamental limits of communication with low probability of detection. *IEEE Trans. Inf. Theory* **2016**, *62*, 3493–3503. [CrossRef]
19. Bash, B.A.; Gheorghe, A.H.; Patel, M.; Habif, J.L.; Goeckel, D.; Towsley, D.; Guha, S. Quantum-secure covert communication on bosonic channels. *Nat. Commun.* **2015**, *6*, 8626. [CrossRef] [PubMed]
20. Tahmasbi, M.; Bloch, M.R. First- and Second-Order Asymptotics in Covert Communication. *IEEE Trans. Inf. Theory* **2019**, *65*, 2190–2212. [CrossRef]
21. Arumugam, K.S.K.; Bloch, M.R. Covert Communication Over a *K*-User Multiple-Access Channel. *IEEE Trans. Inf. Theory* **2019**, *65*, 7020–7044. [CrossRef]
22. Kumar Arumugam, K.S.; Bloch, M.R. Embedding Covert Information in Broadcast Communications. *IEEE Trans. Inf. Forensics Secur.* **2019**, *14*, 2787–2801. [CrossRef]
23. Cho, K.H.; Lee, S.H. Treating Interference as Noise Is Optimal for Covert Communication Over Interference Channels. *IEEE Trans. Inf. Forensics Secur.* **2021**, *16*, 322–332. [CrossRef]
24. Kibloff, D.; Perlaza, S.M.; Wang, L. Embedding Covert Information on a Given Broadcast Code. In Proceedings of the 2019 IEEE International Symposium on Information Theory (ISIT), Paris, France, 7–12 July 2019; pp. 2169–2173. [CrossRef]
25. Tan, V.Y.F.; Lee, S.H. Time-Division is Optimal for Covert Communication Over Some Broadcast Channels. *IEEE Trans. Inf. Forensics Secur.* **2019**, *14*, 1377–1389. [CrossRef]
26. Shahzad, K.; Zhou, X.; Yan, S.; Hu, J.; Shu, F.; Li, J. Achieving Covert Wireless Communications Using a Full-Duplex Receiver. *IEEE Trans. Wirel. Commun.* **2018**, *17*, 8517–8530. [CrossRef]
27. Li, K.; Kelly, P.A.; Goeckel, D. Optimal power adaptation in covert communication with an uninformed jammer. *IEEE Trans. Wirel. Commun.* **2020**, *19*, 3463–3473. [CrossRef]
28. Du, H.; Niyato, D.; Xie, Y.A.; Cheng, Y.; Kang, J.; Kim, D.I. Performance Analysis and Optimization for Jammer-Aided Multiantenna UAV Covert Communication. *IEEE Trans. Wirel. Commun.* **2022**, *40*, 2962–2979. [CrossRef]
29. Wang, Y.; Yan, S.; Yang, W.; Huang, Y.; Liu, C. Energy-Efficient Covert Communications for Bistatic Backscatter Systems. *IEEE Trans. Veh. Commun.* **2021**, *70*, 2906–2911. [CrossRef]
30. Bash, B.A.; Goeckel, D.; Towsley, D. Covert communication gains from adversary's ignorance of transmission time. *IEEE Trans. Wirel. Commun.* **2016**, *15*, 8394–8405. [CrossRef]
31. Chen, W.; Ding, H.; Wang, S.; Gong, F. On the limits of covert ambient backscatter communications. *IEEE Wirel. Commun. Lett.* **2021**, *11*, 308–312. [CrossRef]
32. Abdelaziz, A.; Koksal, C.E. Fundamental limits of covert communication over MIMO AWGN channel. In Proceedings of the 2017 IEEE Conference on Communications and Network Security (CNS), Las Vegas, NV, USA, 9–11 October 2017; pp. 1–9. [CrossRef]
33. Yan, S.; Cong, Y.; Hanly, S.V.; Zhou, X. Gaussian Signalling for Covert Communications. *IEEE Trans. Wirel. Commun.* **2019**, *18*, 3542–3553. [CrossRef]
34. Wang, H.M.; Zhang, Y.; Zhang, X.; Li, Z. Secrecy and Covert Communications Against UAV Surveillance via Multi-Hop Networks. *IEEE Trans. Commun.* **2020**, *68*, 389–401. [CrossRef]